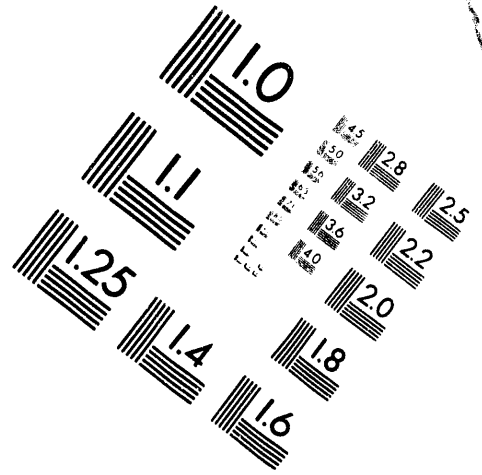
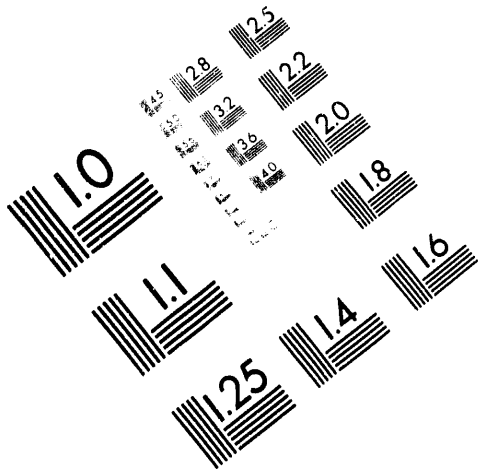




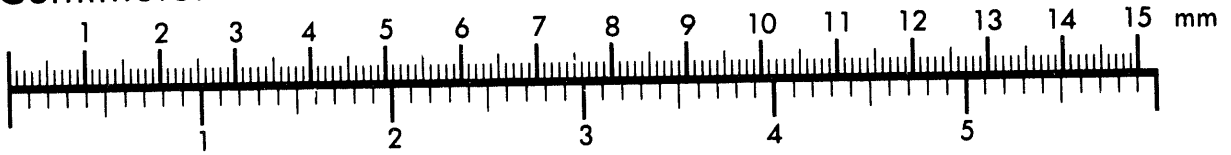
**AIM**

**Association for Information and Image Management**

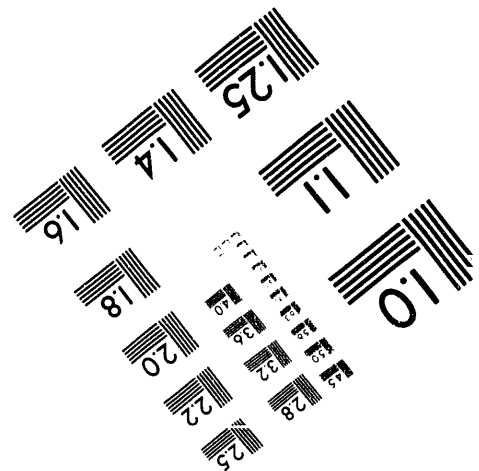
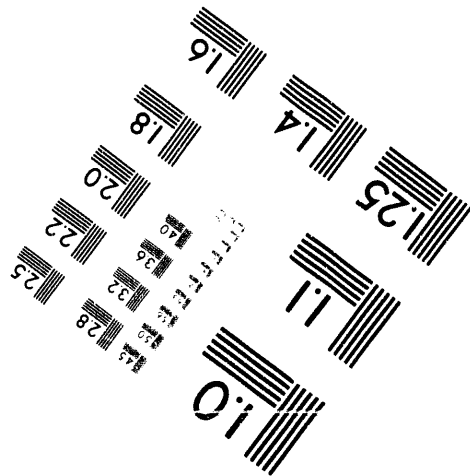
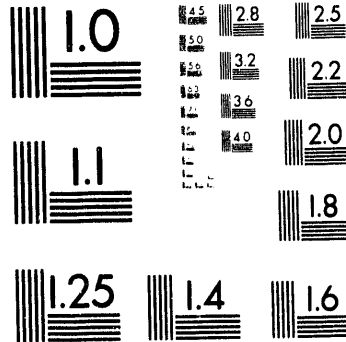
1100 Wayne Avenue, Suite 1100  
Silver Spring, Maryland 20910  
301/587-8202



Centimeter



Inches



MANUFACTURED TO AIM STANDARDS  
BY APPLIED IMAGE, INC.

**1 of 1**

GA-A21310

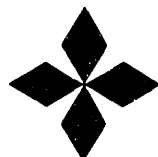
# ANALYSIS OF THE ITER H-MODE CONFINEMENT DATABASE

by  
D.P. SCHISSEL for  
The H-Mode DATABASE WORKING GROUP

This is a preprint of a paper to be presented at the  
20<sup>TH</sup> EPS Conference on Controlled Fusion and  
Plasma Physics, July 26-30, 1993, Lisboa, Portugal  
and to be printed in the *Proceedings*.

Work supported by  
U.S. Department of Energy  
Contract DE-AC03-89ER51114

GENERAL ATOMICS PROJECT 3466  
MAY 1993



**GENERAL ATOMICS**

MASTER

sp

# ANALYSIS OF THE ITER H-MODE CONFINEMENT DATABASE\*

H-MODE DATABASE WORKING GROUP<sup>†</sup>  
PRESENTED BY D.P. SCHISSEL

In order to predict the global energy confinement time in the next generation of large tokamaks it is essential to have data from machines of different sizes and operating parameter regimes. This data can also be used to construct dimensionless scalings and thereby attempt to differentiate between Bohm and gyro-Bohm based transport models. Previously,<sup>1</sup> at the request of the ITER project, H-mode global confinement data was assembled from six machines ASDEX, DIII-D, JET, JFT-2M, PBX-M, and PDX into a single database (DB1). This collaboration has continued<sup>2</sup> with the initial database being expanded by extending the plasma parameter space as well as by improving the precision of some of the relevant calculated plasma parameters. This paper summarizes work that has been performed on the newest version (ITERH.DB2) of the confinement database.

The main emphasis of the recent confinement database work has been to extend and improve the quality of the database as well as improve the analysis. The DB2 confinement database consists of 5998 records of which 3433 are in the H-mode phase. Previously,<sup>1</sup> a standard selection set of H-mode discharges was selected from DB1 for regression analysis. The philosophy of that standard DB1 selection has been continued with DB2 and combined with some additional data constraints which reflect the extended data range that DB2 represents. The DB2 standard selection (1627 records) which has been specified concurrently with the public release of DB2 may be easily reproduced by utilizing the SELDB2 attribute.<sup>2</sup> This standard selection includes only neutral beam heated H-mode discharges and, of those, excludes any time slices with high radiation ( $P_{rad}/P_T > 0.6$ ), with large fast particle content ( $W_f/W_T > 0.4$ ), with transient behavior ( $0.35 > \dot{W}_T/P_T$  or  $< -0.05$ ), with degraded confinement at "low  $q$ ", with operation near the  $\beta$  limit, with hot ion operation, and with pellet injection. In comparison with the selection set used in Ref. 3, the ICRH and combined ICRH/NBI heated discharges from JET have been excluded. Additionally, the JET pulses from 1987 ( $\approx 20$  time slices) have been eliminated from the standard selection set because they have a much larger uncertainty on absorbed power than the other JET pulses. It must be emphasized that there has been no restriction on wall material or evaporation so that discharges with plasma facing composition of stainless steel, Inconel, carbon, and beryllium have been combined into one dataset. To restrict the standard selection to any one of these materials would unacceptably remove a substantial piece of the database.

With respect to DB1, the data in DB2 has been improved by increasing the accuracy of the thermal confinement ( $\tau_{th}$ ) through better estimates of the fast ion content.<sup>3</sup> Moreover, efforts have been made to take into account the effect on confinement of open versus closed divertor tokamaks and different wall conditioning techniques. The ASDEX data in DB2 is with a closed divertor and various wall conditioning techniques. The normalization of ASDEX confinement has already been discussed in detail<sup>3</sup> and remains the same for the present analysis. The JET data normalization previously performed<sup>3</sup> is no longer required since that data has been removed from the standard selection set. The normalization factors for the ASDEX confinement values are now available from the database.

The previous work<sup>3</sup> on normalizing ELMing PDX confinement has been expanded for this study; the normalizations for the PDX confinement are also in the database. PDX ELMing confinement increases with increasing  $R_{D\alpha}^{pds}$  where  $R_{D\alpha}^{pds}$  is defined as the ratio of the divertor to mid-plane  $D_\alpha$  emission. This ratio can be used as a measure of the neutral particle retention of the divertor where a large  $R_{D\alpha}^{pds}$  indicates a closed divertor. The PDX ELMing confinement has been normalized in the database as  $\tau_{th}/(R_{D\alpha}^{pds}/R_{D\alpha}^{tok})^{0.4}$ . The term  $R_{D\alpha}^{tok}$  is a constant for all

---

\* DIII-D work was supported at General Atomics by the U.S. Department of Energy under Contract No. DE-AC03-89ER51114.

<sup>†</sup> ASDEX: O.J.W.F. Kardaun, F. Ryter, U. Stroth, A. Kus; DIII-D: J.C. DeBoo, D.P. Schissel, G. Bramson; JET: K. Thomsen, J.G. Cordey, J.P. Christiansen; JFT-2M: Y. Miura, N. Suzuki, M. Mori, T. Matsuda, H. Tamai, T. Takisuka, S.-I. Itoh, K. Itoh; PBX-M and PDX: S.M. Kaye.

tokamaks and is intended to describe the  $R_{D\alpha}^{pdx}$  if the PDX divertor had the same properties as another tokamak whose  $R_{D\alpha}^{pdx} = R_{D\alpha}^{tok}$ . Therefore, when  $R_{D\alpha}^{pdx}$  is the same as  $R_{D\alpha}^{tok}$  there will be no confinement correction. The exponent 0.4 has been calculated<sup>3</sup> from the PDX ELMing data in DB2. It is not possible to quantitatively determine how a PDX discharge with an "open" divertor corresponds to a similar "open" divertor from another tokamak. Therefore, it is not possible from a physical basis to determine the value of  $R_{D\alpha}^{tok}$ . Instead,  $R_{D\alpha}^{tok}$  has been determined by including this term in the standard regression and minimizing the root mean square error (RMSE). The result from this regression (Fig. 1) is a value of  $\sim 2$  for  $R_{D\alpha}^{tok}$  which is at the lower end of the PDX data range. In our previous study<sup>3</sup> the value of  $R_{D\alpha}^{tok}$  had been set to 3.0.

Having determined the standard DB2 selection set and corrected the ASDEX and PDX confinement values we now determine the ELM-free and ELMing power law scalings. For the ELM-free subset of 858 observations the power law model regression yields (RMSE of 12.3%)

$$\tau_{th} = 0.036 I_p^{1.06} B_T^{0.32} P_L^{-0.67} n_e^{0.17} M^{0.41} R^{1.90} a^{-0.11} \kappa^{0.66} \quad (1)$$

with units of s, MA, T, MW,  $10^{19} \text{ m}^{-3}$ , and meters (Fig. 2). The exponent uncertainties (one standard deviation from ordinary least squares) are 0.03, 0.04, 0.02, 0.02, 0.03, 0.06, 0.04, and 0.05 respectively. The loss power  $P_L$  represents the auxiliary plus Ohmic power minus shinethrough, unconfined orbit, and charge exchange losses and the  $W_T$  correction. For the ELMing dataset (769 observations) the RMSE is 13.8% and the scaling is (Fig. 3)

$$\tau_{th} = 0.022 I_p^{0.76} B_T^{0.15} P_L^{-0.70} n_e^{0.42} M^{0.30} R^{2.30} a^{0.30} \kappa^{1.05} \quad (2)$$

The exponent uncertainties are 0.03, 0.04, 0.02, 0.02, 0.03, 0.08, 0.05, and 0.05 respectively. It should be noted that all types of ELMs have been included in the ELMing dataset.

Realizing that the choice of  $R_{D\alpha}^{tok}$  was both unavoidable and physically arbitrary, it is prudent to examine the sensitivity of the regression result on our numerical choice. Increasing the PDX confinement data by 10% has a considerable effect on the  $R$  and  $\kappa$  scaling (change of  $R^{-0.18} \kappa^{-0.14}$ ). However, this sensitivity is not enough to easily produce an  $R$  scaling similar to that obtained with the ELM-free data. The strong  $R$  scaling in the ELMing compared to ELM-free scaling has been previously observed.<sup>1,3</sup> It should be stated that, in the present database, no clear dependence of the PDX ELM-free confinement on  $R_{D\alpha}^{pdx}$  can be determined and therefore no normalization has been attempted. However, the normalization is less important in the ELM-free case since only 22 time slices are involved compared to 91 in the ELMing dataset.

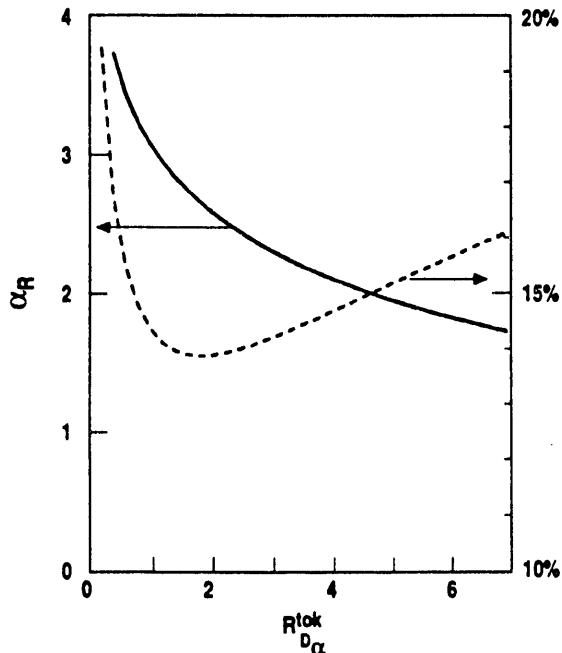


Fig. 1. The parametric dependence of the  $R$  scaling and the RMSE versus  $R_{D\alpha}^{tok}$ .

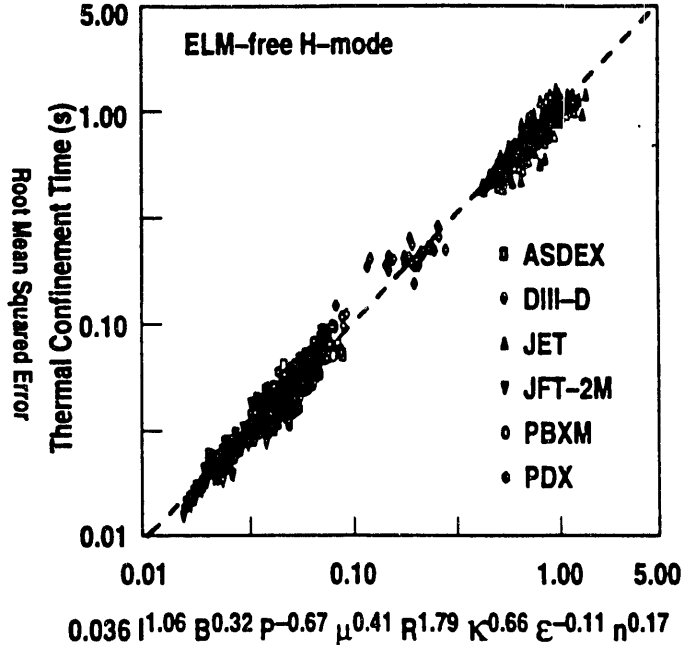


Fig. 2. Observed  $\tau_{th}$  versus that predicted from Eq. (1) for the ELM-free standard dataset.

To investigate the robustness of the ELMing scaling we base a scaling on all tokamaks except JET and utilize this new scaling to predict JET confinement. If the JET ELMing data is removed from the standard selection set the ELMing scaling (681 observations) becomes

$$\tau_{th} = 0.023 I_p^{0.76} B_T^{0.13} P_L^{-0.68} n_e^{0.40} M^{0.30} R^{2.20} a^{0.28} \kappa^{1.00} \quad (3)$$

with an RMSE of 13.6%, which is quite similar to Eq. (2). The exponent uncertainties are 0.04, 0.04, 0.02, 0.03, 0.03, 0.10, 0.06, and 0.05 respectively. Figure 4 displays the observed ELMing JET confinement data against the predictions from Eq. (3). The JET data are in general well predicted. However, there is a band of JET data that is under predicted by about 20%. We do not know the reason for this split. Deleting the JET data increases the sensitivity of the regression to the PDX confinement data (change of  $R^{-0.28} \kappa^{-0.13}$  for a 10%  $\tau_{th}$  increase). Setting the value of  $R_{D_a}^{tok}$  to 3,  $\mu_s$  in Ref. 3, reduces the ELMing  $R$  scaling to  $R^{1.7}$  (Fig. 1).

Although the two ELMing scalings [Eqs. (2) and (3)] are similar it is interesting to note the different JET current scaling between the ELM-free and ELMing data. The JET subset of the standard selection set has  $\tau_{th} \sim I_p^{0.90} n_e^{0.30} B_T^{0.35} P_L^{-0.7}$  for the ELM-free data and  $\tau_{th} \sim I_p^{0.35} n_e^{0.60} B_T^{0.45} P_L^{-0.8}$  for the ELMing data. One notices a weak current dependence in the ELMing data as was previously observed.<sup>5</sup> The very weak JET current scaling must be better understood. One possible explanation behind the weak current scaling is that the high current ELMs are extremely severe, possibly even a return to L-mode, when compared to those from the other tokamaks.

From various considerations, it appears possible that a simple power law representation may not be an adequate model to describe the data. An example of such an occurrence, which was previously investigated,<sup>3</sup> would be when exponents of a simple power law expression are not constant but vary with other plasma parameters. This is called an interaction. Results from JFT2-M<sup>4</sup> show such an effect where the stored energy increases with density at low current but is independent of density at high current. Such interactions can be investigated by adding, on a logarithmic scale, quadratic terms in the simple model. Several potential interaction terms have been investigated within the ELM-free subset of the standard DB2 selection set. Three interaction terms have been found to be significant and shed light on previous work that examined

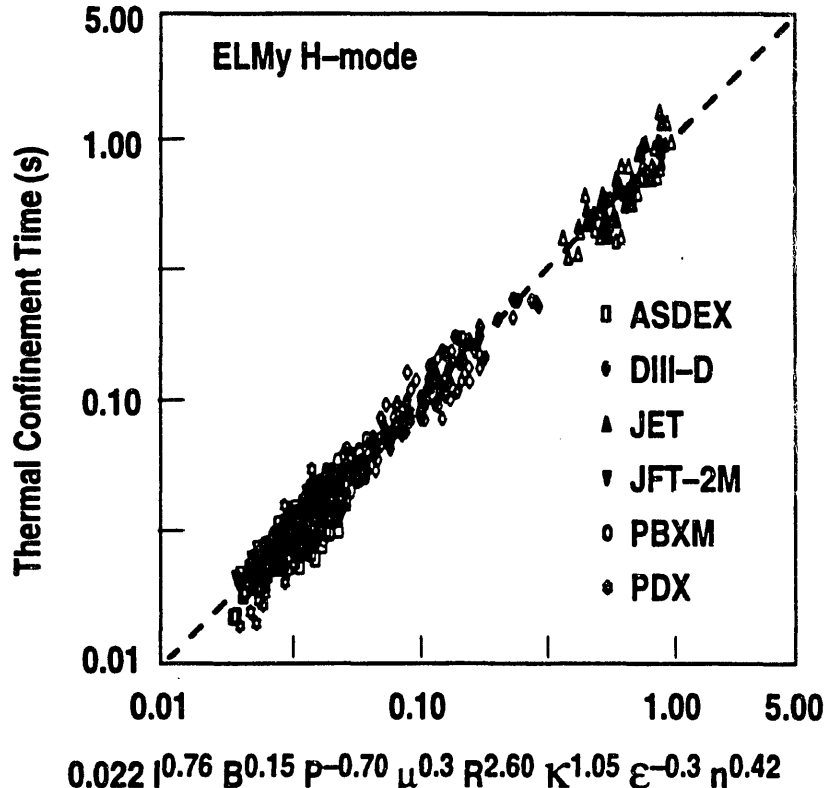


Fig. 3. Observed  $\tau_{th}$  versus that predicted from Eq. (2) for the ELMing standard dataset.

the magnetic field dependence<sup>1</sup> and the  $M$  dependence<sup>3</sup> of confinement. The interaction can be described by

$$\ln(\tau_{th}) = L + 0.3 \ln(n_e) \ln(B_T/j) + 0.1 \ln(j) \ln(P_L/S) + 0.5 \ln(M) \ln(P_L/(n_e V)) \quad (4)$$

where  $L$  denotes the linear terms of a simple power law scaling,  $j$  is the current density ( $I_p/\text{Area}$ ),  $S$  is the plasma surface area, and  $V$  is the plasma volume. This can be interpreted, for example, by writing the effective density exponent as  $\alpha_n^{eff} = \alpha_{n_0} + 0.3 \ln(B_T/j) - 0.5 \ln(M)$ . Note that the  $\alpha_0$  term represents the effective coefficient at one unit (e.g. 1 Tesla, 1 MA/m<sup>2</sup> for a hydrogen plasma) of the regression variables. The RMSE for the ELM-free fit including the interaction terms drops to 11.5%. Our result indicates that as the current increases the density scaling becomes weaker which is consistent with the JFT-2M results.

To examine the implications of our work on the confinement predictions for ITER we consider the CDA design ( $I_p = 22$  MA,  $B_T = 4.85$  T,  $P_L = 200$  MW,  $M = 2.5$ ,  $R = 6$  m,  $a = 2.15$  m,  $\kappa = 2.2$ ,  $n_e = 12.5 \times 10^{19}$  m<sup>-3</sup>) and one of the recent EDA concepts ( $I_p = 25$  MA,  $B_T = 6$  T,  $P_L = 216$  MW,  $M = 2.5$ ,  $R = 7.75$  m,  $a = 2.8$  m,  $\kappa = 1.6$ ,  $n_e = 11 \times 10^{19}$  m<sup>-3</sup>). For the CDA design the  $\tau_{th}$  prediction is  $4.5 \pm 0.7$  s for ELM-free and  $4.8 \pm 0.7$  s for ELMing discharges. The uncertainty represents two standard deviations from ordinary least squares regression. Clearly, given the stated uncertainties, no difference can be inferred between the the ELM-free and ELMing confinement predictions. Recent results from DIII-D<sup>6</sup> indicate an approximate 15% reduction of the ELM-free  $\tau_{th}$  can be expected in the presence of ELMs.

The sensitivity of the ITER predictions to the choice of  $R_{D_0}^{tok}$  is substantial; changing  $R_{D_0}^{tok}$  from 2 to 3 reduces the CDA ELMing confinement from 4.8 s to 3.8 s. For the EDA design, the ELM-free and ELMing confinement predictions are 6.6 s and 6.8 s respectively. Finally, including the three interaction terms increases the ELM-free ITER predictions by approximately 15%;  $\tau_{th}$  is  $5.3 \pm 0.8$  s and  $7.6 \pm 1.2$  s for the CDA and EDA respectively.

Our analysis indicates that the sensitivity of the scalings and ITER predictions to less quantifiable parameters (e.g. divertor type) is significant. Therefore, any attempt to utilize these global scalings to differentiate between a Bohm and a gyro-Bohm type scaling appears difficult. Interaction terms have been found to be significant. This result questions the validity of separating the major plasma parameters into a simple power law expression for  $\tau_{th}$ . Future work should include detailed experimental and physical clarification of the interaction terms.

- 1 Christiansen, J.P., et al., Nucl. Fusion 32 (1992) 291.
- 2 Thomsen, K., et al., to be submitted to Nucl. Fusion.
- 3 Kardaun, O., et al., to be published in Plasma Phys. and Contr. Fusion Research.
- 4 Suzuki, N., et al., Plasma Phys. and Contr. Nucl. Fusion Research, Vol. 1, (1988) 207.
- 5 Kardaun, O., et al., Contr. Fusion and Plasma Phys. (Proc. 16th Euro. Conf. Venice, 1989), Vol. 13B, Part I, EPS (1989) 253.
- 6 Schissel, D.P., et al., Contr. Fusion and Plasma Phys. (Proc. 19th Euro. Conf. Innsbruck, 1992), Vol. 16C, Part I, EPS (1992) 235.

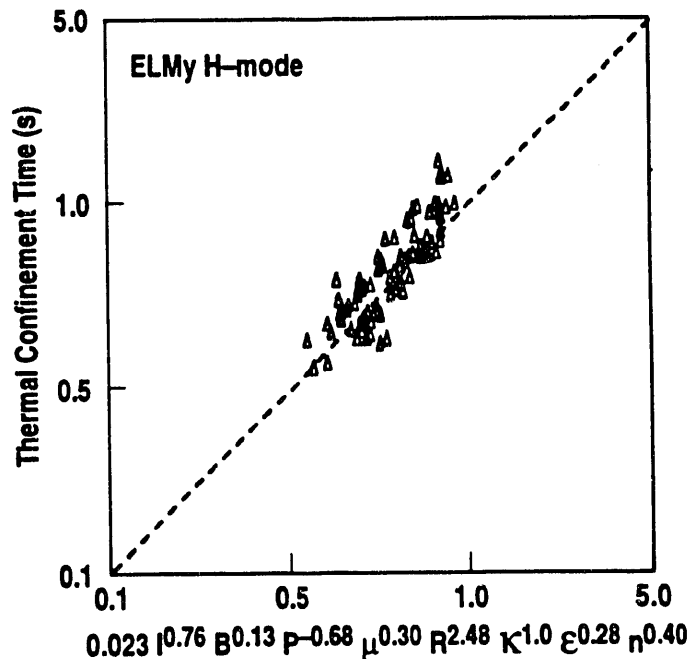


Fig. 4. Observed  $\tau_{th}$  versus that predicted from Eq. (3) for the JET ELMing data. Recall that Eq. (3) is based on all tokamaks except JET.

**DATE**

**FILMED**

9 / 10 / 93

**END**



